BIOCHEMISTRY
including biophysical chemistry & molecular biology

Article

pubs.acs.org/biochemistry

Engineering a Structure Switching Mechanism into a Steroid-Binding Aptamer and Hydrodynamic Analysis of the Ligand Binding Mechanism

Oren Reinstein,[†] Miguel A. D. Neves,[†] Makbul Saad,[†] Sherry N. Boodram,[†] Stephanie Lombardo,[†] Simone A. Beckham,[‡,§] Jason Brouwer,[§] Gerald F. Audette,[†] Patrick Groves,[⊥] Matthew C. J. Wilce,*[,§] and Philip E. Johnson*[,†]

[†]Department of Chemistry, York University, Toronto, Ontario, Canada M3J 1P3

[‡]Centre for Cancer Research, Monash Institute of Medical Research, Monash University, Clayton, VIC 3168, Australia

[§]Department of Biochemistry and Molecular Biology, Monash University, Clayton, VIC 3800, Australia

[⊥]Department of Biological Chemistry, Instituto de Tecnologia Química e Biológica, Av. da Republica (EAN), 2781-901, Oeiras, Portugal

Supporting Information

ABSTRACT: The steroid binding mechanism of a DNA aptamer was studied using isothermal titration calorimetry (ITC), NMR spectroscopy, quasi-elastic light scattering (QELS), and small-angle X-ray spectroscopy (SAXS). Binding affinity determination of a series of steroid-binding aptamers derived from a parent cocaine-binding aptamer demonstrates that substituting a GA base pair with a GC base pair governs the switch in binding specificity from cocaine to the steroid deoxycholic acid (DCA). Binding of DCA to all aptamers is an enthalpically driven process with an unfavorable binding entropy. We engineered into the steroid-binding aptamer a ligand-induced folding mechanism by shortening the terminal stem by two base pairs. NMR methods were used to demonstrate that there is a transition from a state where base pairs are formed in one stem of the free aptamer, to where three stems are formed in the DCA-bound aptamer. The ability to generate a ligand-induced folding mechanism into a DNA aptamer architecture based on the three-way junction of the cocaine-binding aptamer opens the door to obtaining a series of aptamers all with ligand-induced folding mechanisms but triggered by different ligands. Hydrodynamic data from diffusion NMR spectroscopy, QELS, and SAXS show that for the aptamer with the full-length terminal stem there is a small amount of structure compaction with DCA binding. For ligand binding by the short terminal stem aptamer, we propose a binding mechanism where secondary structure forms upon DCA binding starting from a free structure where the aptamer exists in a compact form.

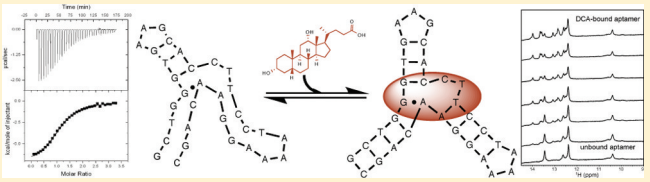

Since their initial development, aptamers have gained widespread use in biosensor applications.[1−3] A large variety of detection methods such as fluorescence, colorimetric, and electrochemical signals have been coupled with aptamer−ligand interactions to indicate the presence of an analyte. In order to produce the maximum desired signal, and therefore greatest sensitivity, ligand binding has been coupled with the occurrence of structural changes in the aptamer that results in the generation of a signal that is detected.[3] A particularly well-developed system for the development of biosensors employing structural switching is that of the cocaine-binding aptamer.[4] Numerous different biosensors have been developed on the basis of the aptamer−cocaine interaction.[5−13] Aside from biosensors, the cocaine-binding aptamer has been employed in supramolecular and nanotechnology applications that take advantage of the structural switching that occurs with ligand binding.[14−16] The common principle among these applications is that cocaine binding assembles separate DNA molecules in a desired and controlled manner. Doubtlessly, the widespread development and use of these applications are limited by the legal and regulatory restrictions placed on the use of the required ligand, cocaine.

The cocaine-binding aptamer is composed of three stems arranged around a three-way junction (Figure 1a).[4] Three variations of the cocaine-binding aptamer have been studied, two of which follow a structural switching or ligand-induced folding mechanism. In the first type of cocaine-binding aptamer, all of the three stems are 4−6 base pairs long (Figure 1a). Here, the aptamer has its secondary structure formed in the free state and binds cocaine with affinity in the low micromolar range depending on the exact sequence and buffer conditions.[5,17,18] The second type of cocaine-binding aptamer consists of stem 1 being shortened to three base pairs (Figure 1b). In this molecule, little secondary structure is formed in the free aptamer and ligand binding prompts secondary structure

Received: August 29, 2011
Revised: September 25, 2011
Published: September 26, 2011

ACS Publications © 2011 American Chemical Society

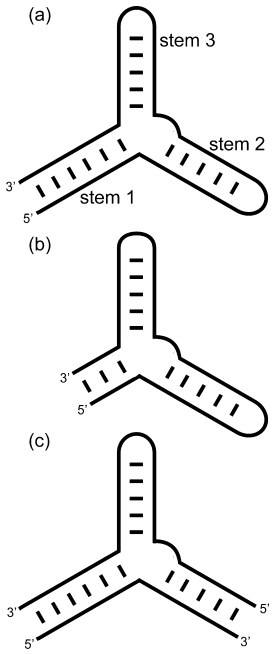

Figure 1. Cocaine-binding aptamers of different sequences and structures show different ligand binding mechanisms. (a) Cocaine-binding aptamers with a stem 1 that is 5−6 base pairs long have their secondary structure preformed. (b) Cocaine-binding aptamers with stem 1 three base pairs long have little secondary structure in the absence of ligand and fold into the shown secondary structure when bound. (c) The cocaine-binding aptamer can be separated into two strands and retain function. In the presence of ligand, the two strands form a ternary complex with cocaine.

formation.[5,11,17−19] Finally, in the third type of cocaine-binding aptamer, the molecule is divided into two separate strands (Figure 1c). In this split aptamer, the two strands interact weakly in the absence of cocaine, but the addition of cocaine drives assembly of the two strands.[4,18,20]

The three-way junction that forms the structural and functional core of the cocaine-binding aptamer has a strong similarity to that of a steroid binding aptamer.[21] Subsequently, the bases at the three-way junction of the cocaine aptamer have been modified to result in sets of biosensors with a range of affinity and specificity for alkaloids as well as steroids such as deoxycholic acid (DCA; Figure 2b).[22−24] This versatility in ligand specificity is uncommon among aptamers and prompted our investigation to see if the different aptamers for the different ligands built around a common DNA architecture follow a similar binding mechanism. With this knowledge it may be possible to alter an aptamer that binds a steroid or other alkaloid to also perform structural switching upon ligand binding. The existence of such a ligand-induced folding mechanism would open up to widespread adoption the biotechnology applications that utilize the ligand-induced folding mechanism of the cocaine-binding aptamer.

MATERIALS AND METHODS

Materials. Aptamer samples were obtained from either Integrated DNA Technologies or the University of Calgary DNA Service. DNA samples were dissolved in water and then exchanged three times in a 3 kDa molecular weight cutoff concentrator with sterilized 1 M NaCl and then washed at least three times with distilled deionized H_2O. Except where noted, all DNA samples were exchanged with buffer A (20 mM Tris (pH 7.4), 140 mM NaCl, 5 mM KCl) three times before use. Aptamer concentrations were determined by absorbance spectroscopy using the calculated extinction coefficients. Sodium deoxycholate (DCA) was obtained from Sigma-Aldrich (part number D6750). Stock solutions of DCA were prepared by weight and dissolved in the desired buffer.

NMR Spectroscopy. 1D ^{1}H NMR experiments on aptamer samples were acquired using a 600 MHz Bruker Avance spectrometer. All 1D ^{1}H NMR spectra were acquired in 90% H_2O/10% ^2H_2O at 5 °C unless otherwise noted. These sample conditions were chosen to result in spectra showing the sharpest signals.[18] Aptamer concentration for NMR studies ranged from 0.3 to 1.5 mM. 2D NOESY spectra were processed and analyzed using NMRPipe/NMRDraw.[25]

Diffusion ordered spectra (DOSY) were acquired according to the protocol described in Groves et al.[26] Samples of the WC aptamer both free and DCA-bound were 0.5 mM in buffer A in ^2H_2O. Spectra were acquired on a Bruker Avance III fitted with a triple resonance probe and Great 50/10 gradient synthesizer (53.5 G/cm maximum output). The ledbpgs2s pulse sequence was used with values of 400 ms for the diffusion delay (D20, big delta, Δ) and 2 ms for the bipolar diffusion gradient (p30, little delta, δ = 4 ms). A series of 32 spectra were stepped linearly over the 2−95% gradient range and processed with Topspin 3.1 software. After processing into an 8K × 1K matrix, columns containing the projected diffusion parameters were summed to create the diffusion profiles. The diffusion profiles were summed in the 7.5−8.5 ppm range for all DNA samples in order to avoid contributions from any free ligand. A set of calibration data were collected at 298 K using the standards aprotinin, α-lactalbumin, carbonic anhydrase, ovalbumin, and bovine serum albumin. The radius of gyration for these proteins was determined from the appropriate pdb file using the VEGA WE online server.[27]

Isothermal Titration Calorimetry. Isothermal titration calorimetry (ITC) was performed using a MicroCal VP-ITC instrument, and the data were analyzed using the accompanying Origin software fit to a one-site binding model. Samples were degassed before use with the MicroCal Thermo Vac unit. All experiments were corrected for the heat of dilution of the titrant. Unless otherwise specified, DCA and aptamer solutions were prepared in buffer A. Binding experiments were performed with aptamer solutions ranging from 20 to 85 μM using DCA concentrations of 1.2−4.2 mM at 20 °C. All aptamer samples were heated in a boiling water bath for 3 min and cooled on ice prior to use in a binding experiment to allow the DNA aptamer to anneal. For the affinity determination experiments of all the aptamers, a low-c ITC method was used to enable all conditions to be studied using the same experimental parameters.[28,29] These low-c ITC experiments consisted of 35 successive injections spaced every 300 s where the first injection was 1 μL, the next 20 injections were 3 μL, and the remaining additions were 15 μL going to a 30−50-fold molar excess of DCA. For the data fitting of the low-c ITC experiments, the stoichiometry of the interaction (n) was set to 1.

The isobaric heat capacity (ΔC_p) of DCA-binding for WC and MS2 was determined by measuring the thermodynamics of binding over a temperature range of 5−40 °C in buffer A. The pH of Tris buffer was not corrected for changes due to temperature effects. For these experiments low-c methods were not used. Standard binding experiments consisted of 35

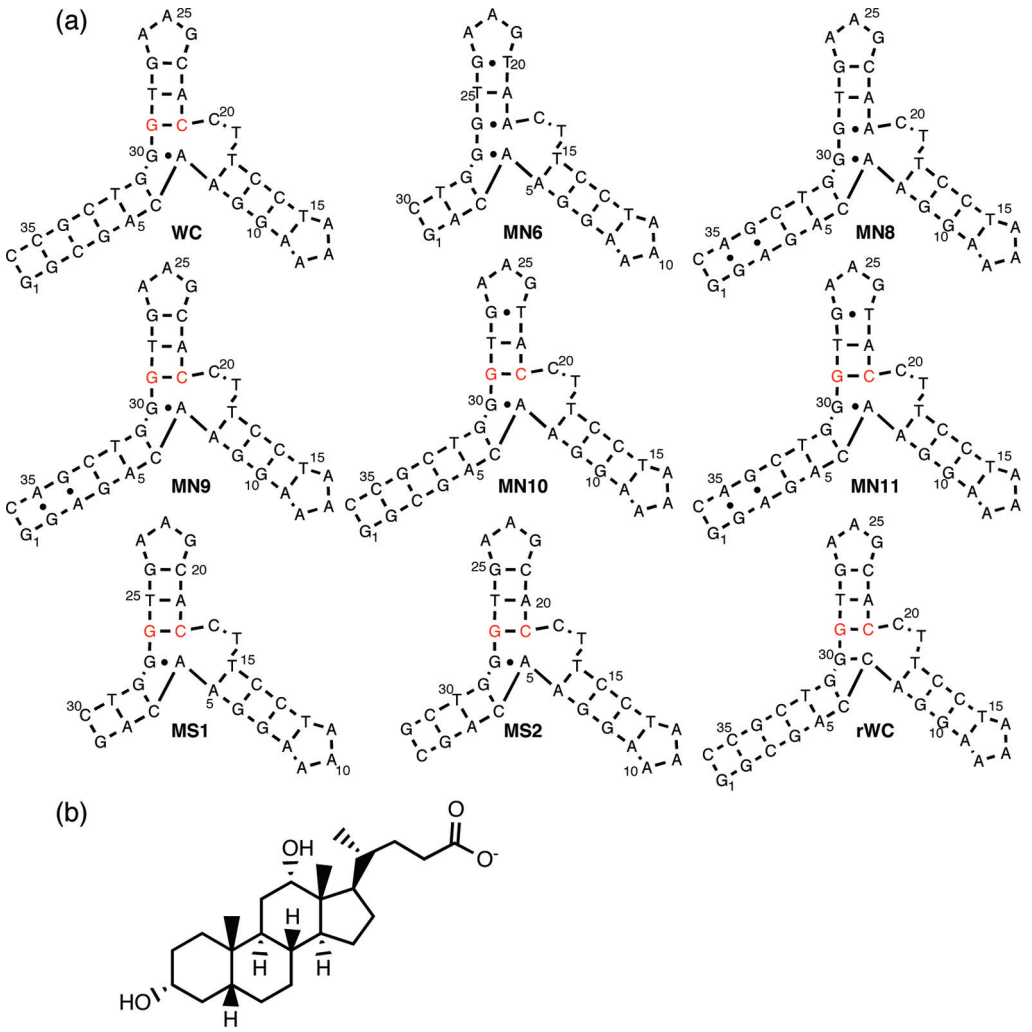

Figure 2. (a) Sequence of the aptamers analyzed in this study. The GC base pair that is important for ligand discrimination between cocaine and DCA binding is shown in red. Dashes between nucleotides indicate Watson–Crick base pairs, and dots indicate non-Watson–Crick base pairs. (b) Chemical structure of deoxycholic acid (DCA).

successive 8 μL injections spaced every 300 s where the first injection was 2 μL. Each experiment had a c value of 5.

Quasi-Elastic Light Scattering. Free and bound WC aptamers were analyzed using SEC-QELS and were performed using an Akta Purifier 10 (GE Healthcare) connected in-line to a Dawn Heleos II and Optilab T-rEX light scattering system (Wyatt Technologies). Analysis of 100 μL of 0.45 mM WC free and DCA bound samples was performed using the same buffer as used for ITC measurements (20 mM Tris (pH 7.4), 140 mM NaCl, 5 mM KCl). After chromatographic separation on a silica-based SEC column (100 Å pore size; Wyatt Technologies), the column eluate traveled to the QELS flow cell where light scattering (658 nm laser light source) by the separated aptamers or aptamers-DCA samples were monitored by 15 angularly separated static light scattering detectors and a quasi-elastic light scattering (QELS) detector at a collection angle of 99°. Hydrodynamic radii (R_h) and diffusion coefficients (D_t) were calculated from an autocorrelation function using the accompanying AstraV software package (Wyatt).

Small-Angle X-ray Scattering. Samples of WC and MS2 aptamers both free and DCA-bound were analyzed using SAXS. Measurements were made using the SAXS-WAXS beamline at the Australian Synchrotron, Melbourne, Australia. Scattering was obtained over a range of four concentrations; the highest concentration was 0.45 and 0.51 mM for the WC and MS2 aptamers, respectively. All SAXS experiments were carried out with the aptamer in buffer A. Scattering data were acquired for the following dilutions: neat sample, 1 in 2, 1 in 4, and 1 in 8. SAXS experiments were performed at room temperature for the WC aptamer and 12 °C for the MS2 aptamer. The samples and matching buffer solutions were exposed to X-ray as the sample flowed through the capillary. The 2D scattering images were normalized for sample transmission and radially averaged. In each case, 20 1-s exposures were recorded and averaged. Scattering from the buffer and empty capillaries was subtracted after scaling scattering intensities to correspond to incident beam intensities. Data analysis was performed using the ATSAS suite of software.[30] Scattered intensity (I) was plotted against s. Extrapolation of the $I(s)$ profiles to zero angle was used to estimate $I(0)$.

RESULTS

Sequence Requirements for Steroid Binding. We used ITC methods to analyze the ability of the WC aptamer and a series of sequence variants (Figure 2a) to bind DCA (Figure 2b). An example of the ITC binding data is shown in Figure 3.

dx.doi.org/10.1021/bi201361v | Biochemistry 2011, 50, 9368–9376

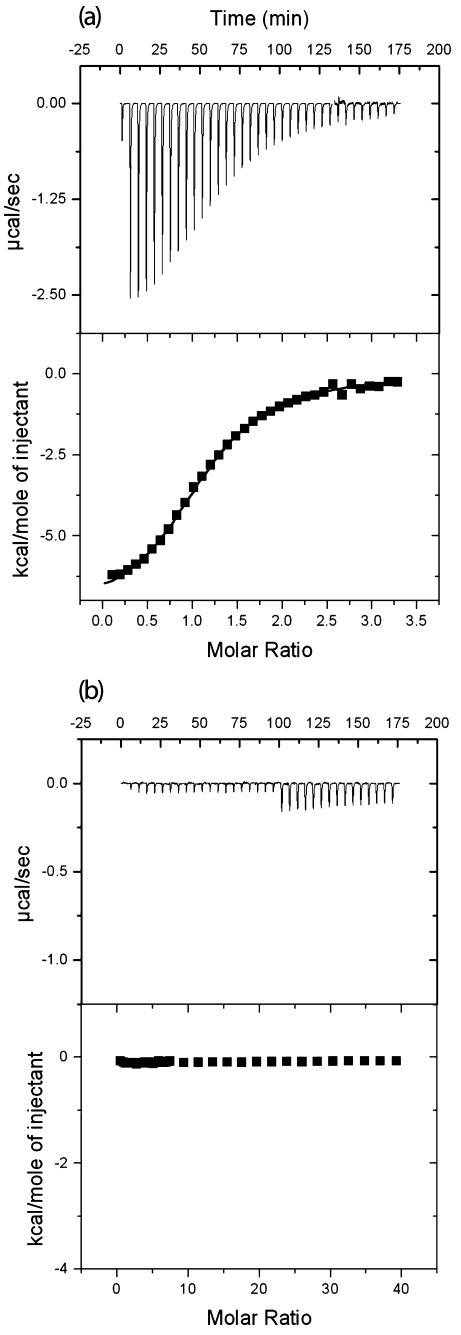

Figure 3. Sample of ITC data showing the interaction of the (a) WC and (b) MN6 aptamers with DCA. In (a) the WC aptamer binds DCA with a K_d value of 16 ± 3 μM while in (b) binding is not detected between MN6 and DCA. On top are the raw titration data showing the heat resulting from each injection of DCA into an aptamer solution. On the bottom are the integrated heats after correcting for the heat of dilution. Binding experiments were performed at 20 °C in a buffer of 20 mM Tris (pH 7.4), 140 mM NaCl, 5 mM KCl.

The affinity and thermodynamic parameters of DCA binding for these constructs are summarized in Table 1. We include the corresponding affinity data for cocaine binding in Table 1 for comparison. From this binding data we observe a trend where constructs with a cytosine corresponding to position 21 of the WC aptamer, and its equivalent position in other constructs (MN9, MN10, MN11), bind DCA with affinity of 12–19 μM. These same aptamers only weakly bind cocaine. Constructs with an adenine in this position, corresponding to position 21 of WC, are able to bind cocaine but do not bind DCA. Sequence changes outside of the vicinity of the tandem GA mismatch in the aptamer have little impact on ligand binding. The WC, MN9, MN10, and MN11 constructs contain different combinations of the GT and GA non-Watson–Crick base pairs observed in the originally selected cocaine-binding aptamer.[4] All these aptamers show similar affinity for DCA and uniformly weak affinity for cocaine. We analyzed the importance of the presence of both GA mismatches for DCA binding using the aptamer rWC. In this aptamer, both GA mismatches were changed to GC base pairs. No binding to either DCA or cocaine was observed for this aptamer. Together, these data indicate that the determinants for ligand selectivity lie at the tandem GA mismatch at the three-way junction.

Table 1. Thermodynamic Parameters and Dissociation Constants of DCA Binding for the Aptamers Presented in This Study[a]

	DCA			cocaine[b]
aptamer	K_d (μM)	ΔH (kcal mol^{-1})	$-T\Delta S$ (kcal mol^{-1})	K_d (μM)
WC	16 ± 3	−7 ± 1	0.7 ± 1.3	204 ± 6
MN6		nbd		45.3 ± 0.5
MN8		nbd		8.6 ± 0.2
MN9	12.2 ± 0.8	−3.7 ± 0.3	2.8 ± 0.1	193 ± 1
MN10	18.6 ± 0.1	−8.4 ± 0.8	2.1 ± 0.8	148 ± 1
MN11	15.0 ± 0.8	−5.2 ± 0.8	1.2 ± 0.8	123 ± 22
rWC		nbd		nd
MS1		nbd		nd
MS2	25 ± 3	−16 ± 1	10 ± 1	nd

[a]Data acquired in 20 mM Tris (pH 7.4), 140 mM NaCl, 5 mM KCl. Data for WC, MS1, and MS2 were acquired at 15 °C; all others were acquired at 20 °C. The values reported are averages of 2–4 individual experiments. The error range reported is one standard deviation. nbd indicates no binding detected. nd indicates that binding for that combination was not measured. [b]The corresponding data for cocaine binding are included for comparison.[18]

Effect of Ionic Strength on DCA Binding. At the pH value these studies were performed (7.4) we expect the DCA to be negatively charged due to the presence of the carboxylate group (Figure 2b). The effect of this negative charge on ligand binding was studied by measuring the affinity and thermodynamics of DCA binding as a function of NaCl concentration. The DCA-binding parameters for the WC aptamer at NaCl concentrations of 0, 140, and 1000 mM are summarized in Table 2. For this aptamer, DCA affinity is tightest at 140 mM NaCl. At both higher and lower NaCl values affinity is weaker. At all three NaCl concentrations, binding remains enthalpically driven with an unfavorable entropy of binding.

Table 2. Dissociation Constant and Thermodynamics of DCA Binding by the WC Aptamer as a Function of NaCl Concentration[a]

[NaCl] (mM)	K_d (μM)	ΔH (kcal mol^{-1})	$-T\Delta S$ (kcal mol^{-1})
0	68 ± 2	−9.0 ± 0.7	3.5 ± 0.7
140	16 ± 3	−7 ± 1	0.7 ± 1.3
1000	46 ± 5	−8 ± 1	2 ± 1

[a]Data acquired at 15 °C in 20 mM Tris (pH 7.4), 5 mM KCl. The values reported are averages of 2–4 experiments.

Engineering of a DCA-Induced Folding Mechanism in an Aptamer with a Short Stem 1. Cocaine-binding

dx.doi.org/10.1021/bi201361v | Biochemistry 2011, 50, 9368–9376

aptamers with a three base pair long stem 1 exhibit a ligand-induced folding mechanism (Figure 1b).[17,19] We designed a DCA-binding aptamer that undergoes a similar unfolded to folded secondary structure transition upon ligand binding. We first tested a modified version of the WC aptamer that has a stem 1 that is three base pairs long (MS1; Figure 2a). No DCA binding was detected by either ITC or NMR methods upon the addition of the ligand (Table1). 1D ^{1}H NMR spectra of MS1 indicate this sequence is unfolded in both the absence and presence of DCA (Figure 1 of the Supporting Information). We then lengthened stem 1 in MS1 by one base pair to make it four base pairs long (MS2; Figure 2a). The resulting MS2 aptamer binds DCA with affinity of 25 ± 3 μM (Table 1).

We used NMR spectroscopy to check the extent of secondary structure formation in the free and bound MS2 as a function of increasing DCA concentration (Figure 4a). In the free MS2, the imino region of the 1-D ^{1}H NMR shows 4 peaks that are assigned to the stem 3 nucleotides G27, T28, G29, and G30 (Figure 2 of the Supporting Information). Upon addition of DCA, there is a significant change in the imino region as numerous additional peaks appear. The appearance of 6−8 additional dispersed peaks indicates the formation of additional secondary structure elements upon ligand binding. Of particular note is the presence of the upfield imino at 10.4 ppm, indicating the presence of a sheared GA base pair in the aptamer.[17] Addition of DCA to WC results in a number of resonances changing chemical shift when ligand binding occurs, but the same number of peaks is observed in the DCA-bound WC aptamer as in the free aptamer.

We then analyzed the stability of the DCA-bound MS2 aptamer using NMR spectroscopy. The 1D ^{1}H NMR spectra of the imino region of the DCA-bound MS2 recorded as a function of temperature are shown in Figure 4b. As the temperature increases for the DCA-bound MS2, two separate groups of transitions are evident. In the first, the group of dispersed peaks that appear with DCA binding and are indicative of a structure containing three stems disappear by 15 °C. The second subset of peaks corresponds to the nucleotides in stem 3, and are those observed in the free MS2. These signals gradually lose intensity and are not visible after 35 °C.

Change in Heat Capacity with Steroid Binding. In order to gain further insight into the DCA binding mechanism and compare it with the cocaine binding mechanism, we used ITC methods to measure the change in heat capacity (ΔC_p) of both WC and MS2 aptamers with DCA binding (Figure 5). For both the WC and MS2 aptamers binding DCA, data obtained at temperatures between 5 and 15 °C were used to determine ΔC_p. Data acquired at higher temperatures were not used as the effects of aptamer folding and unfolding complicate the data. For MS2, we know from the temperature-dependent NMR spectra (Figure 4b) that this aptamer−DCA complex has a temperature of thermal denaturation of ∼20 °C. In the plot of enthalpy versus temperature (Figure 5), the measured enthalpy for MS2 reflects both folding and binding events. A fit of these data for MS2 yields a ΔC_p value of −753 ± 200 cal mol^{-1} K^{-1} for MS2 binding DCA. For the WC aptamer, the measured enthalpy between 5 and 15 °C reflects the binding of the folded free-aptamer to the DCA ligand. A fit of the enthalpy data at these temperatures yields a ΔC_p° value of −94 ± 75 cal mol^{-1} K^{-1}.

Hydrodynamic Analysis Using Quasi-Elastic Light Scattering. Initial analysis of the hydrodynamic properties of free and bound WC was performed using QELS in batch mode. We observed that the DCA-bound WC showed a small but consistent decrease in the translational diffusion coefficient (D_t) when compared to the free aptamer. These initial results were subsequently confirmed using QELS analysis following size exclusion chromatography (SEC-QELS). For the free WC aptamer, SEC-QELS provided a D_t value of (1.12 ± 0.02) × 10^{-8} cm^2 s^{-1}, corresponding to a $R_h(z)$ 28 ± 1 Å. For the DCA-bound WC aptamer SEC-QELS resulted in a D_t value of (1.16 ± 0.02) × 10^{-8} cm^2 s^{-1} and an $R_h(z)$ 26 ± 1 Å (Table 3).

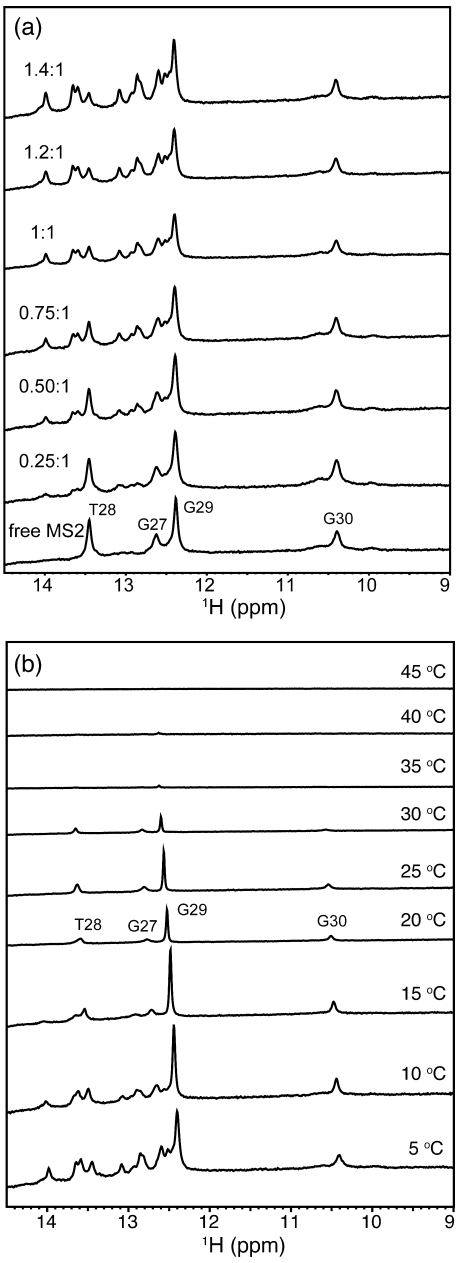

Figure 4. (a) Binding of DCA by the MS2 aptamer demonstrated by 1D ^{1}H NMR spectra. Shown is the region of the NMR spectrum focusing on the imino resonances as a function of increasing DCA concentration. Spectra were acquired in 90% H_2O/10% ^2H_2O at 5 °C. The molar ratios of DCA:aptamer are indicated. (b) Thermal stability of the DCA-MS2 complex assayed by 1D ^{1}H NMR spectra. Shown is the region of the NMR spectrum focusing on the imino resonances as a function of increasing temperature from 5 to 40 °C. Spectra were acquired in 90% H_2O/10% ^2H_2O.

dx.doi.org/10.1021/bi201361v | Biochemistry 2011, 50, 9368−9376

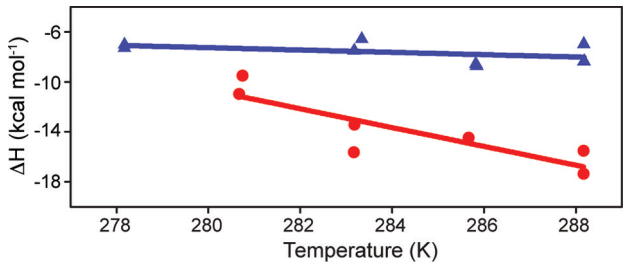

Figure 5. Temperature dependence of the enthalpy of DCA binding for the WC (blue) and MS2 (red) aptamers derived by ITC. The data values are shown while the fit of the data is represented by the solid line. For both aptamers only the low-temperature region where effects of bound aptamer unfolding do not contribute to the enthalpy were used in the fit. Binding experiments were performed in 20 mM Tris (pH 7.4), 140 mM NaCl, 5 mM KCl.

Table 3. Summary of the Hydrodynamic Data for the Free and Bound WC and MS2 Aptamers[a]

	SAXS[b]		DOSY	QELS
sample	R_g (Å)	R_{max} (Å)	R_g (Å)	$R_h(z)$ (Å)
WC_{Free}	17.4 ± 0.1	59.4	17.1	28 ± 1
WC_{bound}	17.6 ± 0.1	60.5	16.3	26 ± 1
$MS2_{Free}$	17.6 ± 0.1	61.0		
$MS2_{bound}$	16.7 ± 0.1	57.2		

[a]Data acquired in 20 mM Tris (pH 7.4), 140 mM NaCl, 5 mM KCl. [b]For SAXS-derived R_g values, data from the 1 in 4 dilution is presented.

Analysis of the Effect of Ligand Binding on Diffusion Using DOSY Methods. In order to analyze any change in molecule shape upon DCA binding, DOSY experiments on the free and ligand-bound WC aptamer were performed. DOSY experiments were performed at temperatures of 5−25 °C. At all temperatures, the log D_t value for the WC-DCA complex was less negative than for the free DCA aptamer (Figure 6; Figure 3 of the Supporting Information). At 25 °C six separate DOSY measurements were performed with the average log D_t value for the free WC aptamer being −9.958 ± 0.002. For the DCA-bound WC at the same temperature the average value of log D_t is −9.939 ± 0.005. This observed decrease in log D_t occurs despite the molecular mass of the complex being heavier than for the free aptamer by the weight of DCA (391.6 Da). This decrease in log D_t likely reflects a small compaction in structure upon ligand binding.

A set of calibration DOSY data was acquired at 25 °C using protein size standards (Figure 6). We used the published three-dimensional structures of the size standards to calculate their respective R_g values in order to get a gauge of the change in molecular size we observed for the WC aptamer upon DCA binding. The standards were aprotinin (pdb id: 1GSX; R_g 11.1 Å), α-lactalbumin (pdb id: 1A4V; R_g 14.8 Å), carbonic anhydrase (pdb id: 1FLJ; R_g 17.5 Å), and ovalbumin (pdb id: 1UHG; R_g 21.9 Å). Bovine serum albumin (66 kDa) was also used as a standard, but no structure for BSA was found. From a plot of log R_g vs log D_t (Figure 4 of the Supporting Information) we estimate the radius of gyration for the free aptamer to be 17.1 Å and that of the bound aptamer to be 16.3 Å (Table 3).

Structural Analysis of DCA Binding Using SAXS. Solution SAXS was conducted on the WC and MS2 aptamers in both the presence and absence of DCA (Figure 7a).

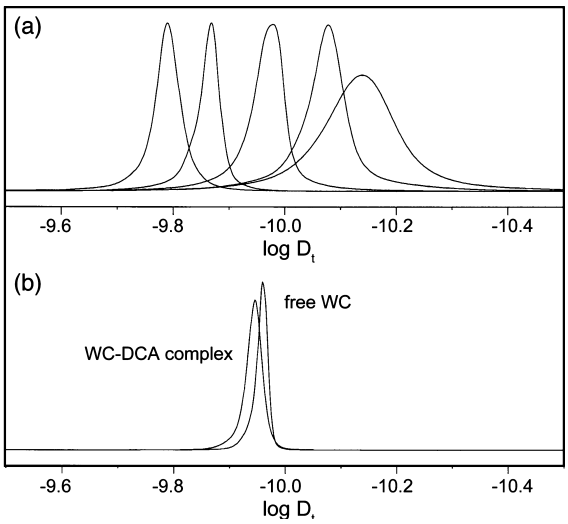

Figure 6. Diffusion profiles obtained from DOSY spectra for, from left to right, (a) aprotinin (6.6 kDa), α-lactalbumin (14.4 kDa), carbonic anhydrase (29 kDa), ovalbumin (44 kDa), and bovine serum albumin (66 kDa). (b) Diffusion profile of free and DCA-bound WC aptamers. The diffusion coefficient of DCA-bound WC aptamer is less negative. This corresponds to a smaller effective molecular weight and smaller R_g, upon complex formation with ligand.

Comparison with water as a standard indicated a molecular mass for all species consistent with no aggregation. The radius of gyration and the maximum dimension of the aptamers are smaller for the neat and 1 in 2 dilution data for each sample (Supporting Information Table 1). This finding is consistent with interparticle interference at these concentrations. The 1 in 4 and 1 in 8 diluted samples have consistent R_g and R_{max} values, and Guinier plots were linear for $sR_g < 1.3$. The 1 in 4 dilution samples were used for all subsequent analysis.

The R_g and R_{max} are similar for both the bound and free aptamers with a slight reduction in both R_g and R_{max} for the ligand-bound MS2 (Table 3). The pair distance distribution function, $P(r)$, was calculated using the indirect Fourier transform method[31] (Figure 7b). The $P(r)$ function is similar for each of the aptamers and is bimodal, having one major peak with a shoulder at r = ~33 Å, and with an extended tail consistent with at least two discrete domains and a slightly elongated molecule. While three of the $P(r)$ functions are essentially the same, there are noticeable differences in the profile of the $P(r)$ function for the WC-DCA sample. The maxima of the curves corresponds to a slightly larger r value, and the shoulder is enhanced indicative of structural changes upon binding DCA. Kratky analysis also suggests that the WC-DCA structure changes upon binding DCA (Figure 7c). Kratky plots for each of the samples are indicative of a partially folded or partially flexible molecule; however, the WC-DCA Kratky plot is suggesting that upon ligand binding WC become more ordered.

DISCUSSION

ITC Analysis of Steroid Binding. The sequence requirement for the change of binding specificity from cocaine to DCA is the single nucleotide replacement of the GA base pair between nucleotides 21 and 29, with a GC base pair (Figure 2a and Table 1). The secondary structure of the cocaine-binding aptamer is comprised of three stems that meet at a three-way junction adjacent to a tandem GA mismatch (Figure 1).[17] The

dx.doi.org/10.1021/bi201361v | Biochemistry 2011, 50, 9368−9376

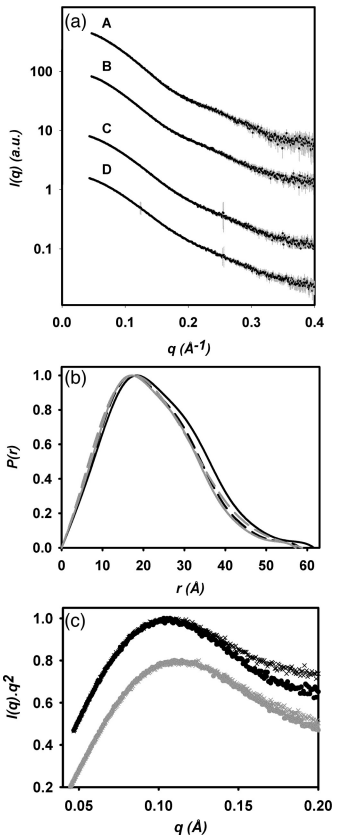

Figure 7. (a) SAXS data for WC and MS2 in the presence and absence of ligand. SAXS intensity profile $I(q)$ as a function of the magnitude of the scattering vector q. Error bars indicate the mean, plus or minus one standard deviation. Line A: WC-DCA; B: free WC; C: MS2-DCA complex; D: free MS2. (b) Pair-distance distribution function ($P(r)$) for WC and MS2 SAXS data. WC-DCA: black solid line; free WC: black dashed line; MS2-DCA: gray solid line; free MS2: gray dashed line. (c) Kratky plot for WC and MS2 SAXS data. WC-DCA: black circles; free WC: black crosses; MS2-DCA: gray circles; free MS2: gray crosses.

identity of the two GA base pairs is critical to retain high affinity cocaine binding.[22,23] As a tandem GA arrangement in a DNA helix is known to distort the helix,[32] it is likely that the disruption of the structure formed by the tandem GA base pairs results in loss of cocaine-binding and conveys DCA-binding ability. Verifying this possible change in structure could be addressed in future studies by employing methods such as SAXS or fluorescence spectroscopy where a 2-aminopurine replaces an adenine to compare a tandem GA-containing aptamer with a WC-type single GA mismatch aptamer.

The WC, MN9, MN10, and MN11 aptamers all bind DCA within a 2-fold range of affinity (Table 1). This demonstrates that nucleotide changes away from the three-way junction have little effect on DCA affinity. In a similar manner, changes outside the three-way junction do not affect cocaine binding.[17,18] We also tested the necessity of the presence of a GA base pair for DCA binding through the use of the rWC construct (Figure 2a). In this molecule, both GA base pairs were changed to GC base pairs, resulting in elimination of DCA binding ability. This finding shows that the presence of a GA base pair is necessary for DCA binding. The sequence requirements to produce a DCA-binding aptamer presented here are consistent with earlier studies that first identified DCA binding by a modified cocaine-binding aptamer with a fluorophore reporter at the three-way junction.[22,23]

The DCA binding mechanism of the WC aptamer was analyzed by measuring the affinity of ligand binding as a function of NaCl concentration. Both the DNA aptamer and the DCA ligand are negatively charged at the pH studied, 7.4. The affinity of the aptamer for DCA is reduced at NaCl concentrations of 0 and 1 M compared to 140 mM NaCl. This finding is in contrast to cocaine binding where the affinity is tightest at 0 M NaCl and indicates that for the WC aptamer electrostatic interactions do not play a positive role in DCA binding by the WC aptamer.

Engineering of a Ligand-Induced Binding Mechanism. We have designed a ligand-induced structural switching binding mechanism to occur in the steroid-binding aptamer MS2. Stem 1 in MS2 is shortened to contain four base pairs, resulting in an aptamer that has secondary structure formed in only stem 3 in the ligand-free state. Upon addition of DCA, numerous well-dispersed resonances appear, indicating the folding of the aptamer into the predicted secondary structure (Figure 4a). The steroid-binding aptamer likely contains the same secondary structural elements seen previously in the cocaine-binding aptamer, indicating that this DNA framework of three stems arranged around a three-way junction appears to be a versatile architecture for ligand binding, and shortening of stem 1 enables the engineering of a structural switching mechanism in a predictable manner.

One difference between the MS2 DCA-binding aptamer and the previously studied MN6 and MN19 cocaine-binding aptamers[17] is that for MN6 and MN19 stem 1 contains three base pairs while for MS2 four base pairs are needed in stem 1 to produce an aptamer that is functional. This suggests that cocaine binding has a greater stabilizing effect than DCA binding. Temperature-dependent NMR experiments demonstrate that, in comparison to cocaine-bound MN6 and MN19, DCA-bound MS2 is less thermally stable. The last of the well-dispersed imino protons that appear in MS2 due to ligand binding are visible at 10 °C, compared to 15 °C for MN6 and MN19.[17] This lower stability exists despite stem 1 having four base pairs in MS2 while MN6 and MN19 have 3 base pairs in their stem 1. While the disappearance of the imino signals can be due to either the unfolding of the aptamer or an increase in the hydrogen exchange rate as the temperature increases, it is clear that DCA binding does not have as much of a stabilizing effect on the MS2 aptamer as cocaine binding has for MN6 and MN19.

One reason why ligand induced folding mechanisms are so useful in analytical methods is that when the biosensor goes from an "off" to an "on" state, the corresponding sensitivity of the signal change is maximized.[3] It should be straightforward to apply the analytical methods based on structural switching in the cocaine aptamer to the steroid binding aptamer sequences presented here. More importantly, new methods that exploit the structural switching mechanism can now be developed using a steroid-binding aptamer as opposed to a cocaine-binding aptamer. Unlike cocaine, there are no legal and regulatory restrictions with using DCA.

Structural Implications of the Hydrodynamic Changes upon Steroid Binding. One aim of this study is to understand what tertiary structure changes occurs with ligand binding by the WC and MS2 aptamers. We addressed this by looking at the changes in hydrodynamics of the free and DCA-bound WC and MS2 aptamers. Additionally, we used

NMR and calorimetry techniques in order to help provide a comparison with our previous findings with the cocaine-binding aptamer.[17,18]

NMR and ITC data indicate a high degree of similarity between the DCA binding mechanisms reported here and the cocaine binding mechanisms described previously.[17−19] The ^{1}H NMR spectrum shows for MS2 only stem 3 is formed in the absence of ligand (Figure 4a, Figure 2 of the Supporting Information), and upon binding DCA, all three stems form (Figure 4a). This behavior is similar to what is seen with short stem 1 variants of the cocaine-binding aptamer.[17] Similarly, the ΔC_p value of MS2 and WC binding DCA show that the short stem 1 variant MS2 has a much more negative ΔC_p value than seen for the WC construct. This indicates that more nonpolar surface area becomes buried upon MS2 binding compared with WC binding which implies that a greater degree of structural change occurs for the short stem 1 constructs than for the long stem 1 aptamers.[33] An additional similarity between the DCA and cocaine binding mechanisms is that for all aptamers studied, binding for both ligands is an enthalpically driven process with an unfavorable binding entropy (Table 1[18]).

For the WC aptamer, we used three different methods to obtain hydrodynamic data that consistently showed that no large-scale tertiary structural changes occur between the free and ligand-bound state. For the DOSY and QELS data, there was evidence of a small increase in the diffusion constant D_t, indicating a small degree of compaction with DCA binding. Using protein size standards, this faster diffusion can be translated into a slightly smaller R_g in the bound WC aptamer compared to the free aptamer (Table 3). For the SAXS data, we observed no significant change in R_g with DCA binding by the WC aptamer. This difference between methods may arise from small changes in the roughly flat elongated shape of the aptamer changing the diffusion rate but still giving rise to the same R_g as measured by SAXS. Despite the lack of difference in R_g values between free and DCA-bound WC, analysis of the SAXS data using the $P(r)$ function and the Kratky plot (Figure 7b,c) indicates the presence of structural changes in the WC aptamer with DCA binding and indicates that the aptamer becomes more ordered upon DCA binding. Together, these results indicate little change in the overall size of the molecule with ligand binding but that structural changes do occur in the WC aptamer with DCA binding. Previously, for cocaine binding, we saw little to no secondary structure change with cocaine binding by the MN4 aptamer,[17] but we did not have a means to look at changes in tertiary structure. Given the similarity in NMR and ITC trends between the cocaine-binding MN4 aptamer and DCA-binding WC aptamers, it is likely that these hydrodynamic findings would be similar for MN4 binding cocaine.

SAXS methods were also used to look at what structural changes occur with DCA binding by the MS2 aptamer. We found a significant decrease in R_g for the MS2 aptamer with ligand binding (Table 3) as may be expected given the secondary structure formation in this aptamer with DCA binding. Surprisingly, there is little difference in the Kratky plot between free and DCA-bound MS2, indicating that MS2 does not become significantly more ordered with ligand binding. This apparent discrepancy with the NMR data that shows secondary structure formation in two stems in MS2 can be best explained if we think about what the structure of the unbound state may look like. If the unbound state exits as an unfolded, random coil, spaghetti-like strand, then secondary structure formation of two stems should represent a large increase in order. However, if the unbound form exists in a compact form, one where the base pairs outside of stem 3 are not yet formed but the strands are already aligned close together, then ligand binding and base pair formation can occur without a large change in order as reflected in the Kratky plot (Figure 8).

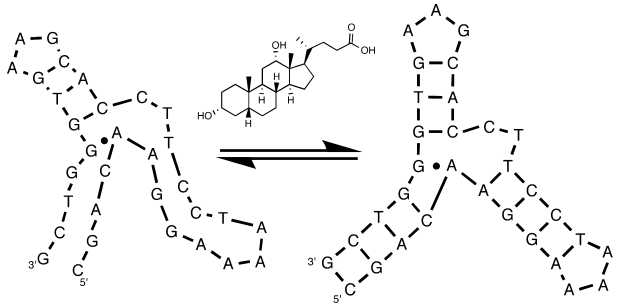

Figure 8. Proposed mechanism for the structural changes that occur with ligand binding by the MS2 aptamer. In the free state stem 3 is formed and the molecule exists in a compact prefolded form where stems 1 and 2 do not exist in a random coil. With ligand binding, base pair formation in stems 1 and 2 take place despite little change in overall order occurring.

In summary, we have engineered a ligand-induced folding mechanism into a steroid binding aptamer. We accomplished this by shortening stem 1 in the DCA-binding aptamer in a similar manner as seen in the cocaine-binding aptamer. Only some fine-tuning of the stem 1 length was needed to achieve a mechanism where two stems of the three-way junction form with ligand binding in the MS2 aptamer. Given the propensity shown by the DNA architecture of the cocaine-binding aptamer to be selective for different ligands,[22−24] it should be possible to use this structure as a general template to obtain a set of aptamers that exhibit ligand-induced folding that is specific to a wide array of ligands.

■ ASSOCIATED CONTENT

Ⓢ Supporting Information

Figures showing the 1D ^{1}H NMR spectrum of the MS1 construct in the presence and absence of DCA, the assignment of the free MS2 imino ^{1}H NMR spectrum, a plot of the DOSY-derived log D_t values versus temperature and the log R_g values versus log D_t values for the size standards; one table containing the SAXS-derived R_g and R_{max} values for the free and DCA-bound WC and MS2 aptamers at all concentrations studied. This material is available free of charge via the Internet at http://pubs.acs.org.

■ AUTHOR INFORMATION

Corresponding Author

*E-mail pjohnson@yorku.ca, phone 416-736-2100 x3319, fax 416-736-5936 (P.E.J.); e-mail matthew.wilce@monash.edu, phone 613-9902-09244, fax 613-9902-9500 (M.C.J.W.).

Funding

This work was supported by funding from the Natural Sciences and Engineering Research Council of Canada (NSERC); The Portuguese National NMR Network (REDE/1517/RMN/2005) was supported by Programa Operacional Ciência e Inovação 2010 and Fundação para a Ciência e a Tecnologia. M.C.J.W. is a Senior Research Fellow of the National Health and Medical Research Council of Australia and is funded by

both the Australian Research Council and the National Health and Medical Research Council of Australia.

■ ACKNOWLEDGMENTS

We thank Anna Petrov for help with the light scattering experiments and members of the Johnson laboratory (York University, Toronto) for useful discussions.

■ ABBREVIATIONS

ΔC_p, change in heat capacity; DCA, deoxycholic acid; DOSY, diffusion ordered spectroscopy; D_t, translational diffusion coefficient; ITC, isothermal titration calorimetry; K_d, dissociation constant; NMR, nuclear magnetic resonance; R_g, radius of gyration; R_h, hydrodynamic radius; SAXS, small-angle X-ray scattering; SEC-QELS, size exclusion chromatography quasi-elastic light scattering.

■ REFERENCES

(1) Liu, J., Cao, Z., and Lu, Y. (2009) Functional nucleic acid sensors. *Chem. Rev. 109*, 1948−1998.
(2) Cho, E. J., Lee, J.-W., and Ellington, A. D. (2009) Applications of aptamers as sensors. *Annu. Rev. Anal. Chem. 2*, 241−264.
(3) Li, D., Song, S., and Fan, C. (2010) Target-responsive structural switching for nucleic acid-based sensors. *Acc. Chem. Res. 43*, 631−641.
(4) Stojanovic, M. N., de Prada, P., and Landry, D. W. (2000) Fluorescent sensors based on aptamer self-assembly. *J. Am. Chem. Soc. 122*, 11547−11548.
(5) Stojanovic, M. N., de Prada, P., and Landry, D. W. (2001) Aptamer-based folding fluorescent sensor for cocaine. *J. Am. Chem. Soc. 123*, 4928−4931.
(6) Stojanovic, M. N., and Landry, D. W. (2002) Aptamer-based colorimetric probe for cocaine. *J. Am. Chem. Soc. 124*, 9678−9679.
(7) Zhang, J., Wang, L., Pan, D., Song, S., Boey, F. Y. C., Zhang, H., and Fan, C. (2008) Visual cocaine detection with gold nanoparticles and rationally engineered aptamer structures. *Small 4*, 1196−1200.
(8) Madru, B., Chapuis-Hugon, F., Peyrin, E., and Pichon, V. (2009) Determination of cocaine in human plasma by selective solid-phase extraction using an aptamer-based sorbent. *Anal. Chem. 81*, 7081−7086.
(9) Baker, B. R., Lai, R. Y., Wood, M. S., Doctor, E. H., Heeger, A. J., and Plaxco, K. W. (2006) An electronic, aptamer-based small-molecule sensor for the rapid, label-free detection of cocaine in adulterated samples and biological fluids. *J. Am. Chem. Soc. 128*, 3138−3139.
(10) Liu, J., Mazumdar, D., and Lu, Y. (2006) A simple and sensitive "dipstick" test in serum based on lateral flow separation of aptamer-linked nanostructures. *Angew. Chem., Int. Ed. 45*, 7955−7959.
(11) Li, T., Li, B., and Dong, S. (2007) Adaptive recognition of small molecules by nucleic acid aptamers through a label-free approach. *Chem.—Eur. J. 13*, 6718−6723.
(12) Chen, J., Jiang, J., Gao, X., Liu, G., Shen, G., and Yu, G. (2008) A new aptameric biosensor for cocaine based on surace-enhanced raman scattering spectroscopy. *Chem.—Eur. J. 14*, 8374−8382.
(13) Swensen, J. S., Xiao, Y., Ferguson, B. S., Lubin, A. A., Lai, R. Y., Heeger, A. J., Plaxco, K. W., and Soh, H. T. (2009) Continuous, real-time monitoring of cocaine in undiluted blood serum via a microfluidic, electrochemical aptamer-based sensor. *J. Am. Chem. Soc. 131*, 4262−4266.
(14) Freeman, R., Sharon, E., Tel-Vered, R., and Willner, I. (2009) Supramolecular cocaine-aptamer complexes activate biocatalytic cascades. *J. Am. Chem. Soc. 131*, 5028−5029.
(15) Wang, Z.-G., Wilner, O. I., and Willner, I. (2009) Self-assembly of aptamer-circular DNA nanostructures for controlled biocatalysis. *Nano Lett. 9*, 4098−4102.
(16) Freeman, R., Sharon, E., Teller, C., and Willner, I. (2010) Control of Biocatalytic Transformations by Programmed DNA Assemblies. *Chem.—Eur. J. 16*, 3690−3698.
(17) Neves, M. A. D., Reinstein, O., and Johnson, P. E. (2010) Defining a stem length-dependant binding mechanism for the cocaine-binding aptamer. A combined NMR and calorimetry study. *Biochemistry 49*, 8478−8487.
(18) Neves, M. A. D., Reinstein, O., Saad, M., and Johnson, P. E. (2010) Defining the secondary structural requirements of a cocaine-binding aptamer by a thermodynamic and mutation study. *Biophys. Chem. 153*, 9−16.
(19) Cekan, P., Jonsson, E. O., and Sigurdsson, S. T. (2009) Folding of the cocaine aptamer studied by EPR and fluorescence spectroscopies using the bifunctional spectroscopic probe Ç. *Nucleic Acids Res. 37*, 3990−3995.
(20) Sharma, A. K., and Heemstra, J. M. (2011) Small-molecule-dependent split aptamer ligation. *J. Am. Chem. Soc. 133*, 12426−12429.
(21) Kato, T., Yano, K., Ikebukuro, K., and Karube, I. (2000) Interaction of three-way DNA junctions with steroids. *Nucleic Acids Res. 28*, 1963−1968.
(22) Stojanovic, M. N., Green, E. G., Semova, S., Nikic, D. B., and Landry, D. W. (2003) Cross-reactive arrays based on three-way junctions. *J. Am. Chem. Soc. 125*, 6085−6089.
(23) Green, E., Olah, M. J., Abramova, T., Williams, L. R., Stefanovic, D., Worgall, T., and Stojanovic, M. N. (2006) A rational approach to minimal high-resolution cross-reactive arrays. *J. Am. Chem. Soc. 128*, 15278−15282.
(24) Pei, R., Shen, A., Olah, M. J., Stefanovic, D., Worgall, T., and Stojanovic, M. N. (2009) High-resolution cross-reactive array for alkaloids. *Chem. Commun.*, 3193−3195.
(25) Delaglio, F., Grzesiek, S., Vuister, G. W., Zhu, G., Pfeifer, J., and Bax, A. (1995) NMRPipe: A multidimensional spectral processing system based on UNIX pipes. *J. Biomol. NMR 6*, 277−293.
(26) Groves, P., Palczewska, M., Molero, M. D., Batta, G., Cañada, F. J., and Jiménez-Barbero, J. (2004) Protein Molecular weight standards can compensate systematic errors in Diffusion Ordered Spectroscopy. *Anal. Biochem. 331*, 395−397.
(27) Pedretti, A., Villa, L., and Vistoli, G. (2004) VEGA - An open platform to develop chemo-bio-informatics applications, using plug-in architecture and script programming. *J. Comput.-Aided Mol. Des. 18*, 167−173.
(28) Turnbull, W. B., and Daranas, A. H. (2003) On the value of c: can low affinity systems be studied by isothermal titration calorimetry? *J. Am. Chem. Soc. 125*, 14859−14866.
(29) Tellinghuisen, J. (2008) Isothermal titration calorimetry at very low c. *Anal. Biochem. 373*, 395−397.
(30) Konarev, P. V., Volkov, V. V., Sokolova, A. V., M.H.J., K., and Svergun, D. I. (2003) PRIMUS - a Windows-PC based system for small-angle scattering data analysis. *J. Appl. Crystallogr. 36*, 1277−1282.
(31) Svergun, D. I. (1991) Mathematical methods in small-angle scattering data analysis. *J. Appl. Crystallogr. 24*, 485−492.
(32) Gao, Y.-G., Robinson, H., Sanishvili, R., Joachimiak, A., and Wang, A. H.-L. (1999) Structure and recognition of sheared tandem GA base pairs associated with human centromere DNA sequence at atomic resolution. *Biochemistry 38*, 16452−16460.
(33) Spolar, R. S., and Record, M. Jr. (1994) Coupling of local folding to site-specific binding of proteins to DNA. *Science 263*, 777−784.